Supplementary Material

This supplement contains Supplementary Figures 1-10 with legends, and Supplementary References.

Supplementary Figure Legends

Supplementary Fig. 1. Citric acid cycle (CAC) metabolism in 143B*wt* and 143B*cytb* cells. **a,** Proliferation of 143B*wt* and 143B*cytb* cells. Doubling times were 28±1 and 33±2 hrs for 143B*wt* and 143B*cytb* cells, respectively. **b,** Relative abundance of succinate (Succ), fumarate (Fum), malate (Mal) and citrate (Cit) in 143B*wt* and 143B*cytb* cells. Data are the average ± S.D. of three independent cultures. *$p<0.05$, Student's t-test. **c,d,** Mass isotopomers of fumarate and malate in 143B*wt* and 143B*cytb* cells cultured in medium containing D[U-^{13}C]glucose and unlabeled glutamine. The majority of these pools contain no ^{13}C (m+0) because these metabolites are predominantly derived from glutamine, as outlined in Supplementary Fig. 3. The reduced contribution of m+2 in the 143B*cytb* metabolites is consistent with the reduced glucose-derived citrate m+2 in these cells (Fig. 1b). The modest enhancement of m+3 may reflect a small induction of pyruvate carboxylation[1]. Data are the average ± S.D. of three independent cultures. * $p<0.05$, Student's t-test. **e,f,** Mass isotopomers of malate and succinate in cells cultured in medium containing unlabeled glucose and L[U-^{13}C]glutamine. In 143B*cytb* cells, succinate m+4 exceeds succinate m+3. This is different from the mass isotopomer distribution in fumarate and malate (Fig. 1d, Supplementary Fig. 1e), where m+3 > m+4. Thus succinate is formed using both oxidative (producing m+4) and reductive (producing m+3) glutamine e metabolism. Both pathways contribute to the large succinate pool in the 143B*cytb* cells (panel **b**), and defective processing of succinate m+4 to fumarate m+4 is consistent with the known suppression of succinate oxidation in cells with complex III dysfunction[2]. Oxidative metabolism of α-KG to succinate generates reducing equivalents in the form of NADH (by α-KG dehydrogenase). Inefficient recycling of NADH to NAD^+ because of impaired electron transport

chain function in 143B*cytb* cells may contribute to the propensity for reductive carboxylation. Data are the average ± S.D. of three independent cultures. * $p<0.05$, Student's t-test.

Supplementary Fig. 2. Schematic for metabolism of D[U-^{13}C]glucose. Metabolism of D[U-^{13}C]glucose (Glc) produces uniformly ^{13}C-labeled pyruvate (Pyr) and, if pyruvate dehydrogenase (PDH) is active, uniformly ^{13}C-labeled acetyl-CoA (Ac-CoA). In 143B*wt* cells, a large flux from unlabeled glutamine (Gln) fills the CAC from α-ketoglutarate to oxaloacetate (α-KG to OAA). Thus condensation of OAA with Ac-CoA usually produces citrate (Cit) containing two ^{13}C atoms (Cit m+2). Much of this ^{13}C exits the cycle for use in lipid synthesis and other reactions, but some of it is oxidized within the CAC to produce a modest amount of OAA m+2. If this condenses with labeled Ac-CoA, Cit m+4 is produced. In 143B*cytb* cells, little glucose carbon enters the CAC through PDH, reducing the amount of Cit m+2 and m+4 (Fig. 1b). Abbreviations: Glu, glutamate; Succ-CoA, succinyl-CoA; Succ, succinate; Fum, fumarate; Mal, malate; ACL, ATP-Citrate Lyase.

Supplementary Fig. 3. Schematic for metabolism of L[U-^{13}C]glutamine in 143B*wt* and 143B*cytb* cells. In 143B*wt* cells and other cells with normal CAC activity (**top**, green pathway), metabolism of L[U-^{13}C]glutamine produces uniformly ^{13}C-labeled CAC intermediates from α-ketoglutarate to oxaloacetate (αKG to OAA). Condensation of labeled OAA with glucose-derived (unlabeled) Ac-CoA produces Cit m+4, which can exit the cycle. Cleavage by ATP-citrate lyase (ACL) generates unlabeled Ac-CoA, which is used for lipid synthesis, and OAA m+4, which can be metabolized further following any of several routes. Acetyl-CoA can also be produced from glutamine by oxidative decarboxylation of malate to pyruvate (not shown), followed by pyruvate dehydrogenase (PDH) activity. In 143B*cytb* cells and other cells using reductive carboxylation (**bottom**, red pathway), glutamine-derived αKG is reduced to

isocitrate/citrate m+5, incorporating one unlabeled carbon. Cleavage of Cit m+5 produces OAA m+3 (bearing the unlabeled carbon) and uniformly labeled Ac-CoA for lipid synthesis. Subsequent reductive metabolism of OAA m+3 produces additional m+3 CAC intermediates such as malate, fumarate and succinate (Mal, Fum, Succ). In 143B*cytb* cells, there is also oxidative metabolism of α-KG to succinate, producing a succinate pool that is a mixture of m+3 and m+4 isotopomers (Supplementary Fig. 1f). Abbreviations: Glu, glutamate; Succ-CoA, succinyl-CoA; Isocit, isocitrate; αKGDH, αKG dehydrogenase.

Supplementary Fig. 4. Glutamine-dependent reductive carboxylation in Roswell Park Memorial Institute (RPMI) medium. a, Metabolism of D[U-^{13}C]glucose in 143B*wt* and 143B*cytb* cells cultured in RPMI. As in Dulbecco's Modified Eagle Medium (DMEM, Fig. 1b), 143B*cytb* cells displayed a large reduction in the entry of glucose-derived carbon into the citrate pool. **b-d,** Metabolism of L[U-^{13}C]glucose in 143B*wt* and 143B*cytb* cells cultured in RPMI. As in DMEM, 143B*cytb* cells displayed large reductions in citrate/fumarate/malate m+4, and large increases in citrate m+5 and fumarate/malate m+3 consistent with glutamine-dependent reductive carboxylation. All data are the average ± S.D. of three independent cultures.

Supplementary Fig. 5. Glutamine-dependent reductive carboxylation in cells with a defect in Complex I of the ETC. CCL16-B2 Chinese hamster cells contain a truncating mutation in the *NDUFA1* gene, resulting in a severe defect of Complex I activity and respiration[3]. These cells were transduced with the *Saccharomyces cerevisiae* NADH-quinone oxidoreductase, partially restoring respiration[4]. When cultured in L[U-^{13}C]glutamine, CCL16-B2 cells produced predominantly citrate m+5 and fumarate/malate m+3, consistent with reductive carboxylation. These species were suppressed in CCL16-NDI1 cells. Data are the average ± S.D. of three independent cultures.

Supplementary Fig. 6. Subcellular localization of IDH1 and IDH2. a, Immunofluorescence of 143B*wt* and 143B*cytb* cells using antibodies against IDH1 (top panels) or IDH2 (bottom panels. Cells were also transiently transfected with control (Ctrl) siRNAs or siRNAs directed against IDH1 or IDH2 to verify isoform specificity of the antibodies. IDH1 signal was observed diffusely throughout the cytoplasm and did not co-localize with a mitochondrial stain (Mitotracker). By contrast, IDH2 signal occurred in a punctate pattern that co-localized with Mitotracker. **b,** Cytoplasmic and mitochondrial subcellular fractions of 143B*wt* and 143B*cytb* cells were probed for IDH1, IDH2, glyceraldehyde 3-phosphate dehydrogenase (GAPDH, a cytoplasmic control) and succinate dehydrogenase subunit A (SDHA, a mitochondrial control). Abbreviations, DAPI, 4',6-Diamidino-2-Phenylindole; IB, immunoblot.

Supplementary Fig. 7. Growth of pools of 143B*wt* and 143B*cytb* cells after stable silencing of IDH1 or IDH2 using three independent lentiviral shRNAs directed against each isoform. After antibiotic selection, $2x10^5$ cells from each pool were plated, cultured for 72 hours and counted. The number of cells in each shRNA pool was normalized to growth of cells expressing a control shRNA. Data are the average ± S.E.M. for four independent cultures. *$p<0.05$; **$p<0.005$, Student's t-test.

Supplementary Fig. 8. Summary of ^{13}C lipid NMR. a, Four independent experiments each were performed for 143B*wt* and 143B*cytb* cells, two in D[U-^{13}C]glucose + unlabeled glutamine, and two in unlabeled glucose + L[U-^{13}C]glutamine. In each sample of extracted lipids, NMR was used to analyze the contribution of the triplet and doublet to the total area of the multiplet at ω-1. The singlet due to natural abundance ^{13}C signal, which contributed a small fraction of the total area, is not shown. **b,** ^{13}C NMR spectroscopy of UOK262 lipids labeled with D[U-

^{13}C]glucose (left) or L[U-^{13}C]glutamine (right). The contribution of the triplet to total area of the ω-1 multiplet was 17% in D[U-^{13}C]glucose and 60% in L[U-^{13}C]glutamine.

Supplementary Fig. 9: ETC inhibitors rapidly induce glutamine-dependent reductive carboxylation. a, MEFs transformed with SV40 Large T-antigen were cultured for 6 hours in medium containing unlabeled glucose and L[U-^{13}C]glutamine, with or without the ETC inhibitors metformin (10 mM), rotenone (1 μM) and antimycin (1 μM). Data are the mass isotopomer distribution for citrate, average ± S.D. of three independent cultures. *$p<0.05$, Student's t-test. **b,** 143B*wt* cells were cultured in medium containing unlabeled glucose and L[U-^{13}C]glutamine, with or without rotenone, for the indicated duration. Data are the citrate m+5 as a percentage of the total citrate pool. **c,** 143B*wt* cells were cultured with or without 100 μg/mL cycloheximide (CHX) in the presence of unlabeled nutrients for 5 hours, then the medium was replaced with medium containing L[U-^{13}C]glutamine in the presence or absence of CHX and rotenone. The cells were cultured for 2 more hours, then metabolites were extracted and analyzed to analyze reductive carboxylation. CHX pre-treatment blunted but did not eliminate the induction of reductive carboxylation (citrate m+5, left panel). In the same experiment, rotenone increased labeling of glutamate (glutamate m+5, right panel), and this enhancement was completely eliminated by pre-treatment with CHX. Thus the blunted rotenone-mediated increase in citrate m+5 was likely a consequence of effects upstream of IDH, with reduced labeling in substrate pools being transmitted to citrate. The decreased overall labeling in citrate of CHX-treated cells (increased m+0) supports this idea. Data are the mass isotopomer distribution for citrate, average ± S.D. of three independent cultures.

Supplementary Fig. 10: Metformin induces glutamine-dependent reductive carboxylation in a dose-dependent fasion. 143B*wt* cells were cultured in medium containing unlabeled

glucose and L[U-^{13}C]glutamine with the indicated concentrations of metformin for 6 hours. Relevant mass isotopomers are shown for citrate, fumarate and malate.

Supplementary References

1 Cheng, T. *et al.*, Pyruvate carboxylase is required for glutamine-independent growth of tumor cells. *Proc Natl Acad Sci U S A* **108**, 8674-8679 (2011).

2 Slipetz, D.M., Aprille, J.R., Goodyer, P.R., & Rozen, R., Deficiency of complex III of the mitochondrial respiratory chain in a patient with facioscapulohumeral disease. *Am J Hum Genet* **48**, 502-510 (1991).

3 Au, H.C., Seo, B.B., Matsuno-Yagi, A., Yagi, T., & Scheffler, I.E., The NDUFA1 gene product (MWFE protein) is essential for activity of complex I in mammalian mitochondria. *Proc Natl Acad Sci U S A* **96**, 4354-4359 (1999).

4 Seo, B.B. *et al.*, Molecular remedy of complex I defects: rotenone-insensitive internal NADH-quinone oxidoreductase of Saccharomyces cerevisiae mitochondria restores the NADH oxidase activity of complex I-deficient mammalian cells. *Proc Natl Acad Sci U S A* **95**, 9167-9171 (1998).

Supplementary Fig. 1

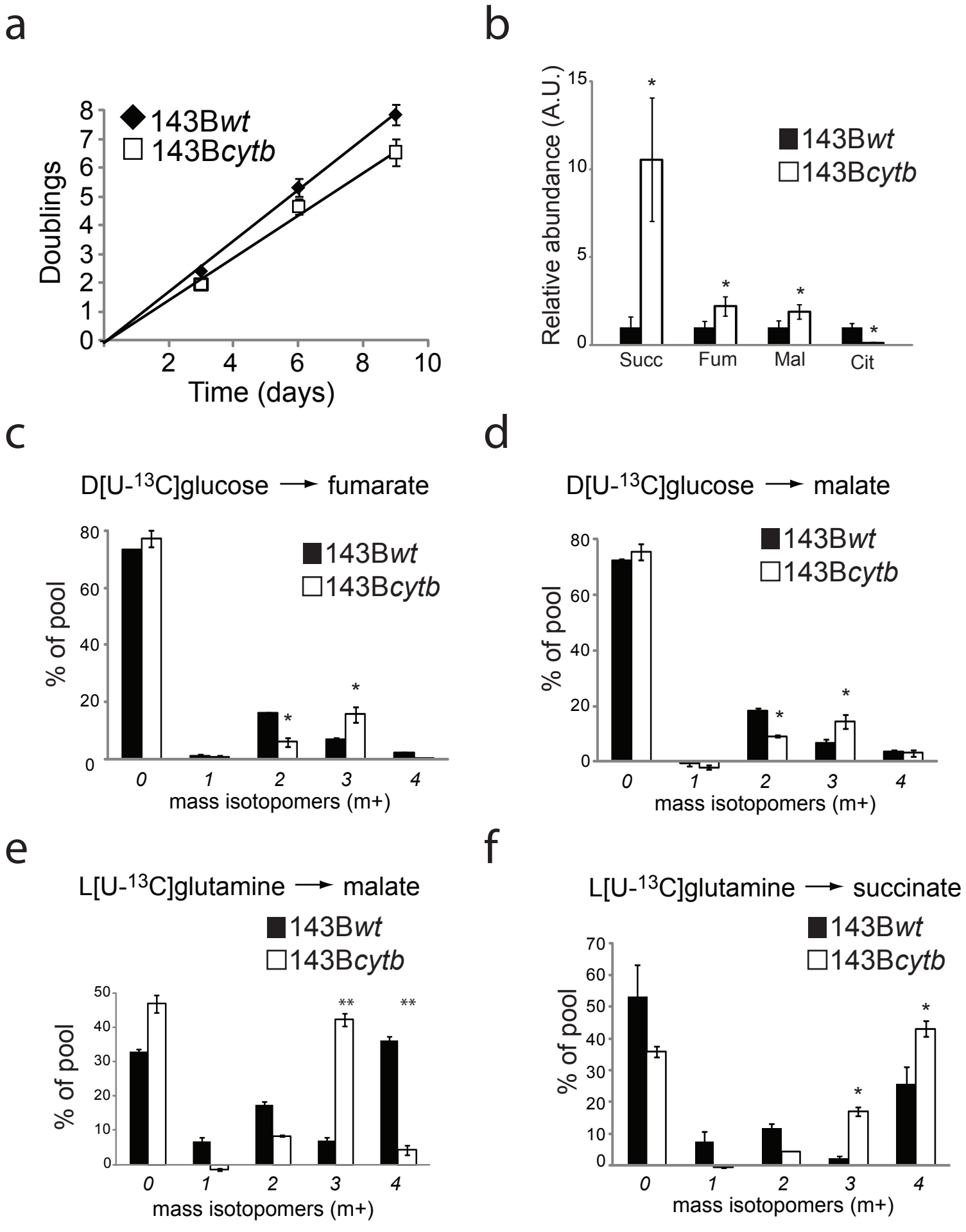

Supplementary Fig. 2

Labeling with D[U-^{13}C]glc

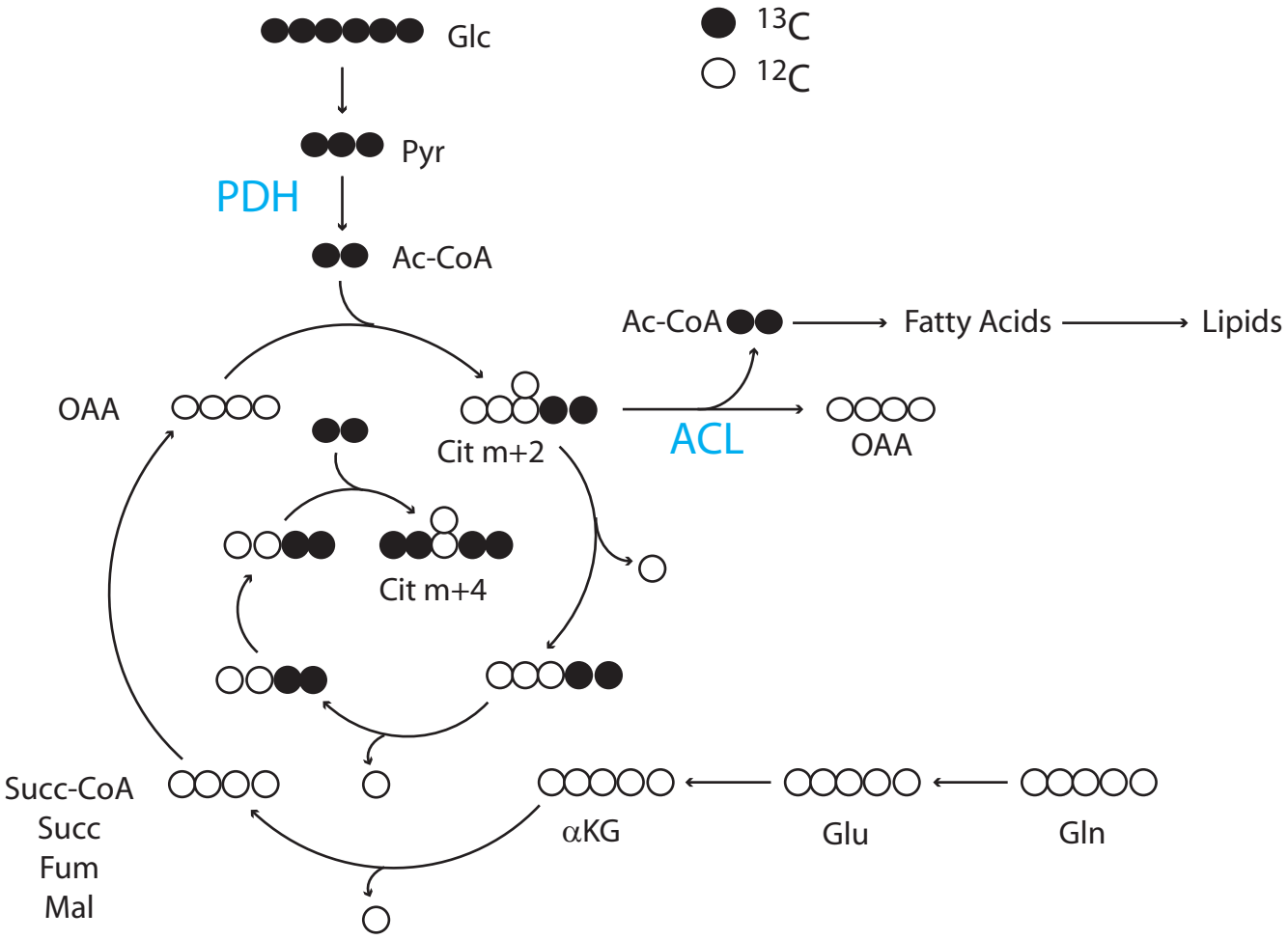

Supplementary Fig. 3

143B*wt* cells

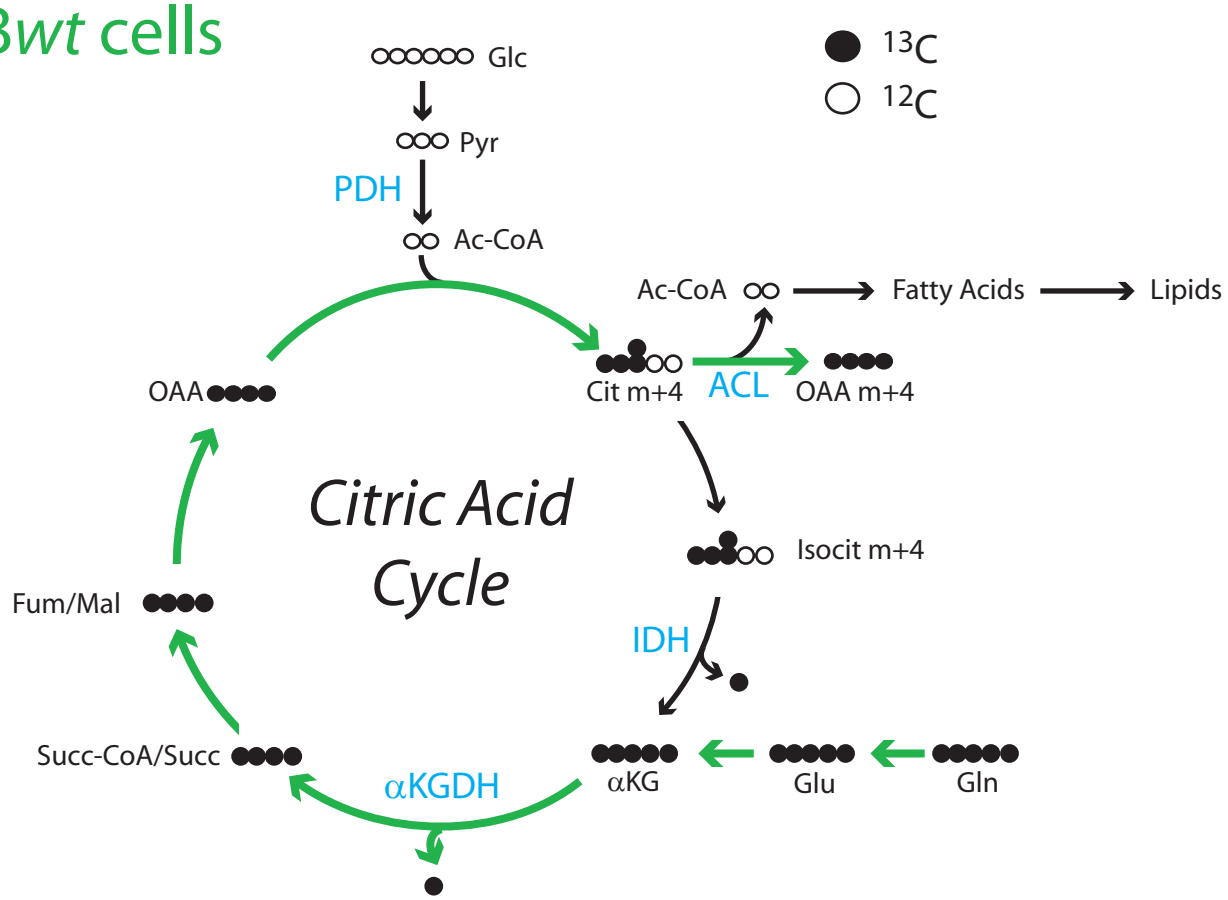

143B*cytb* cells

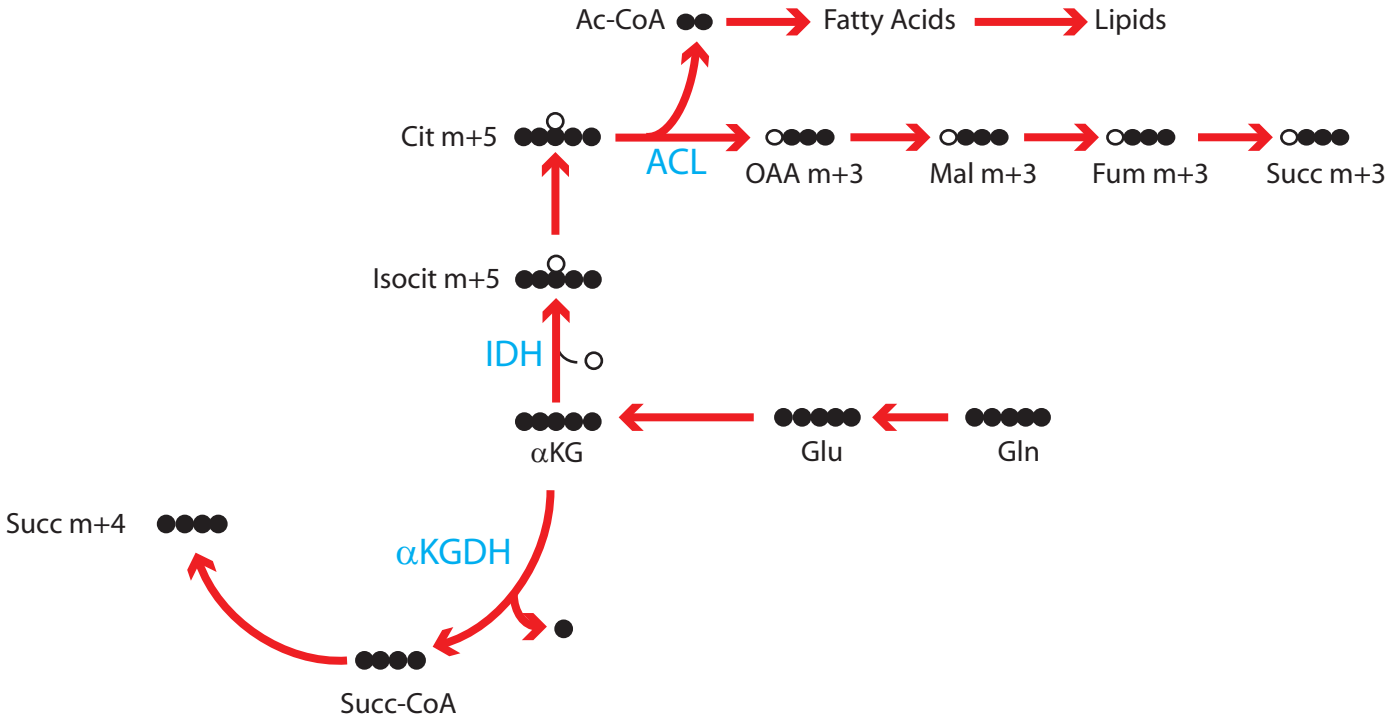

Supplementary Fig. 4

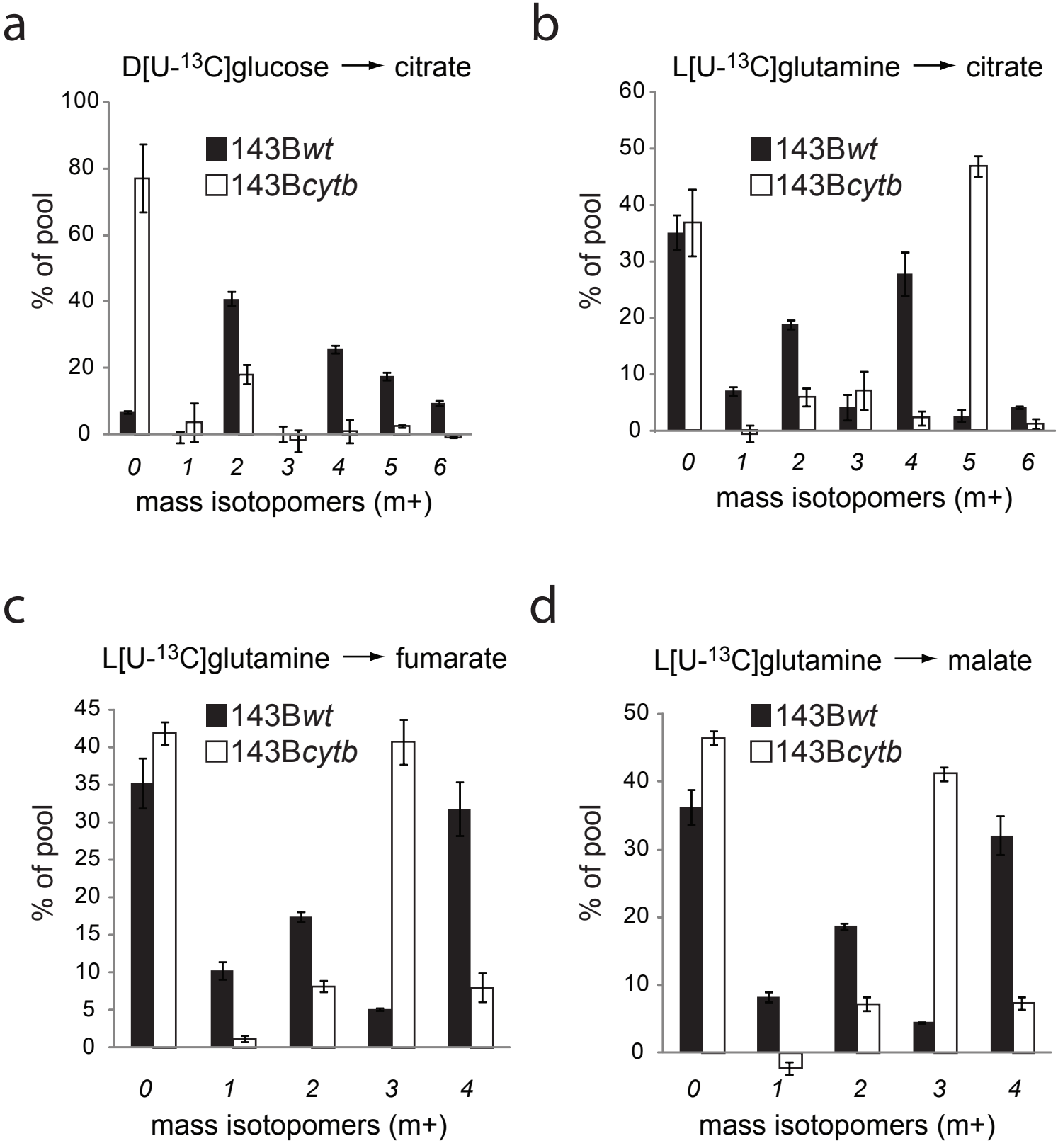

Supplementary Fig. 5

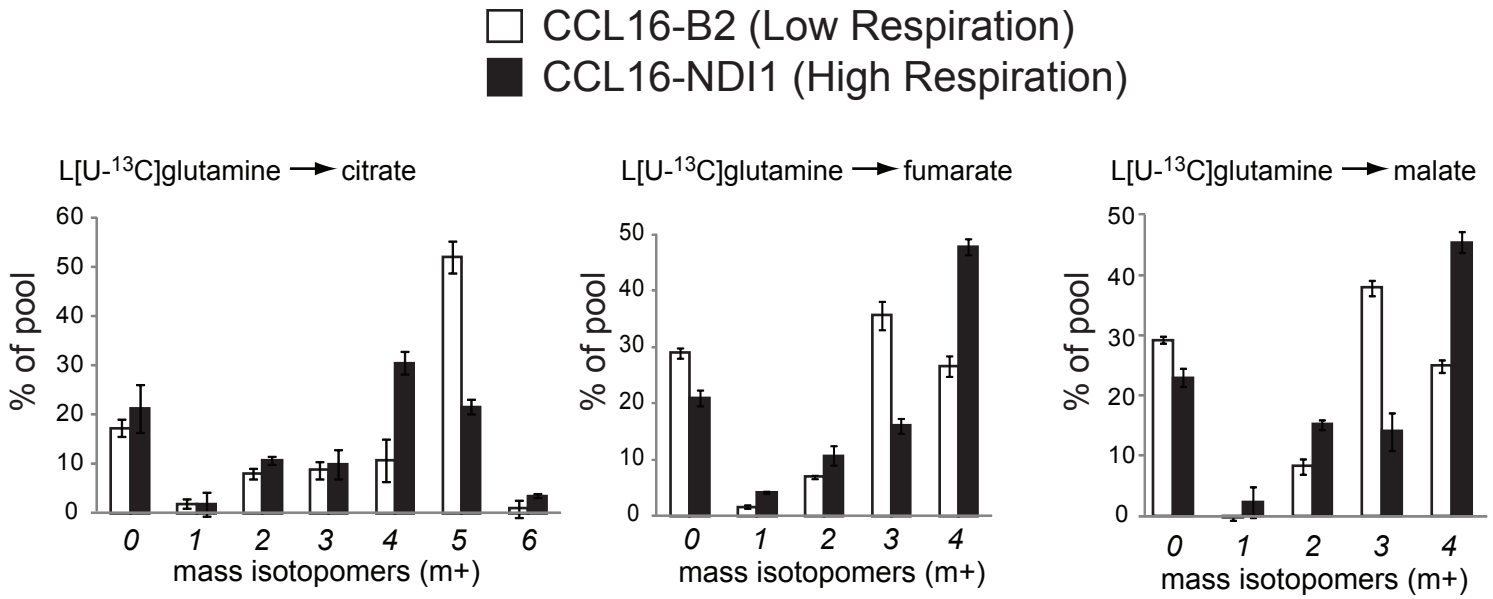

Supplementary Fig. 6

a

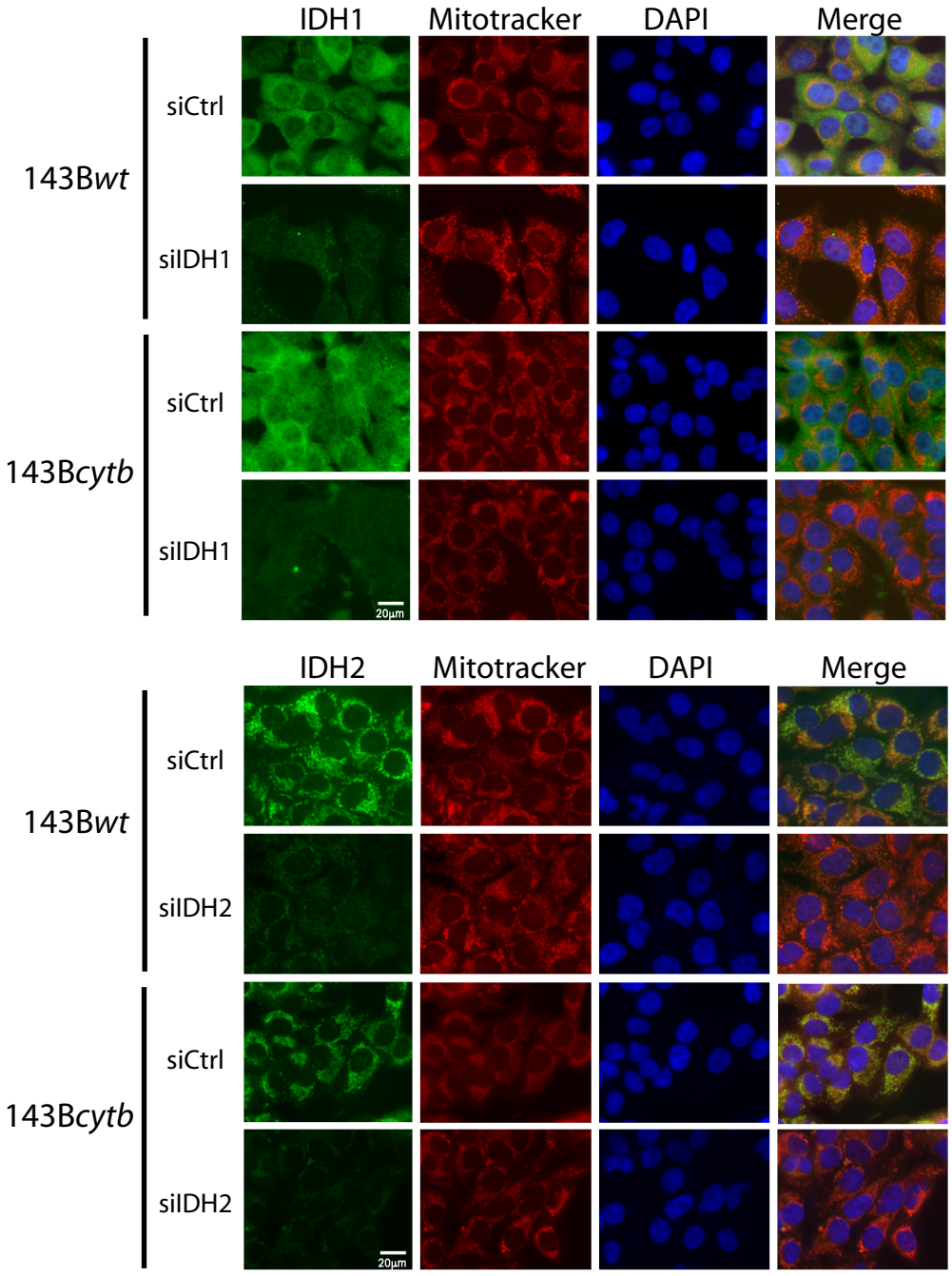

b

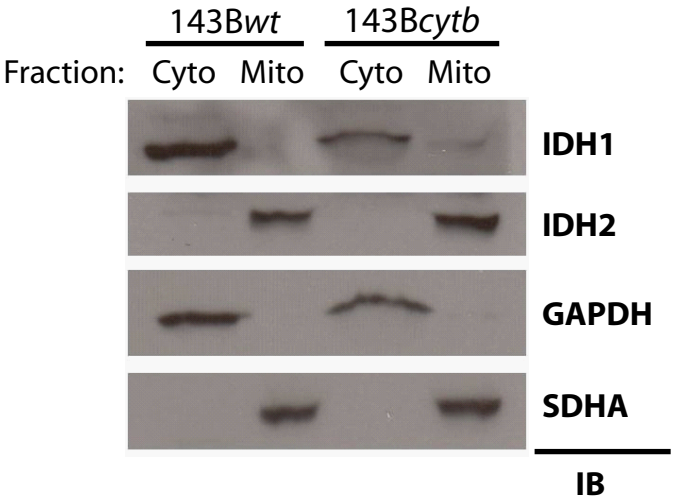

Supplementary Fig. 7

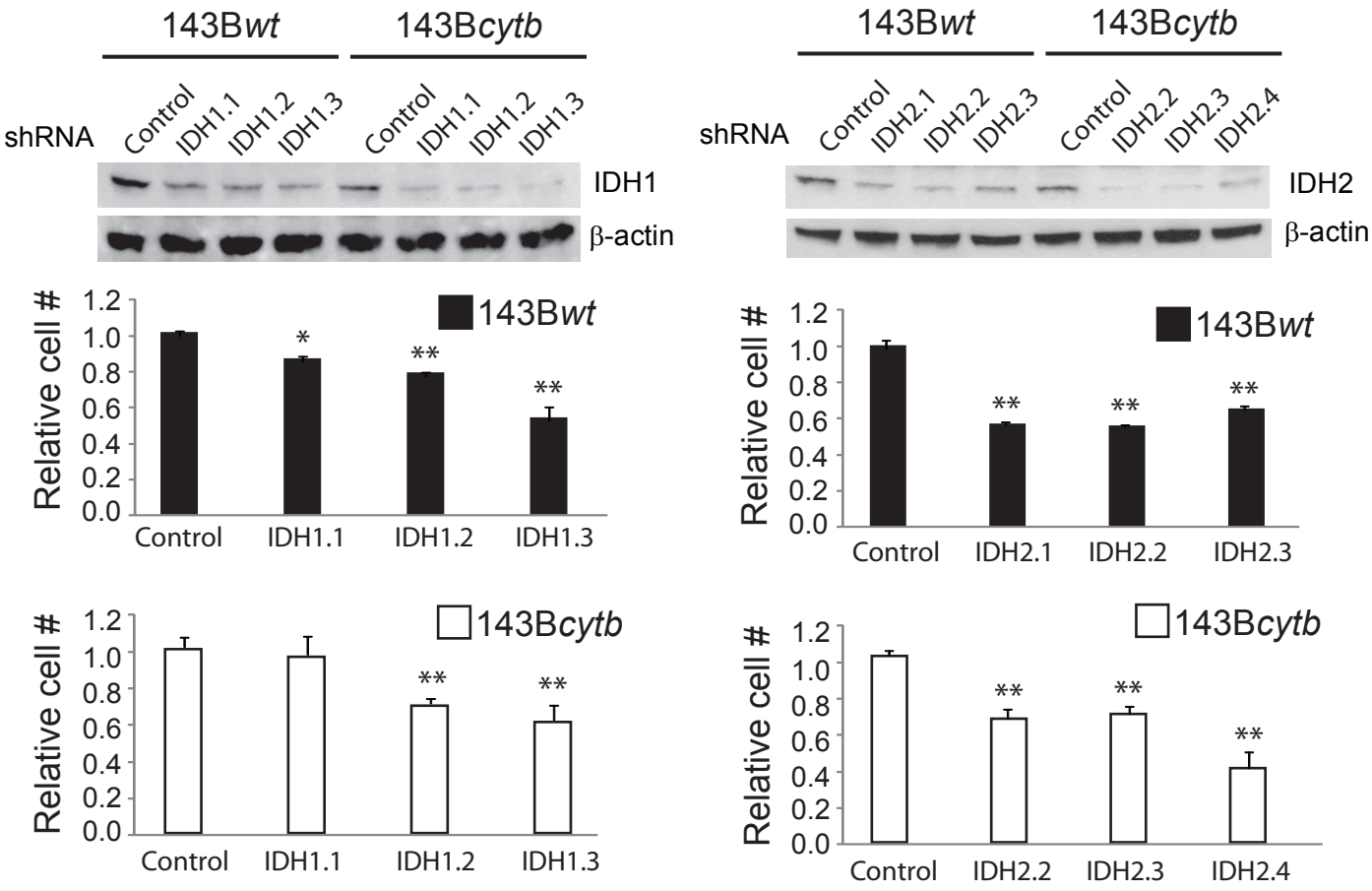

Supplementary Fig. 8

a

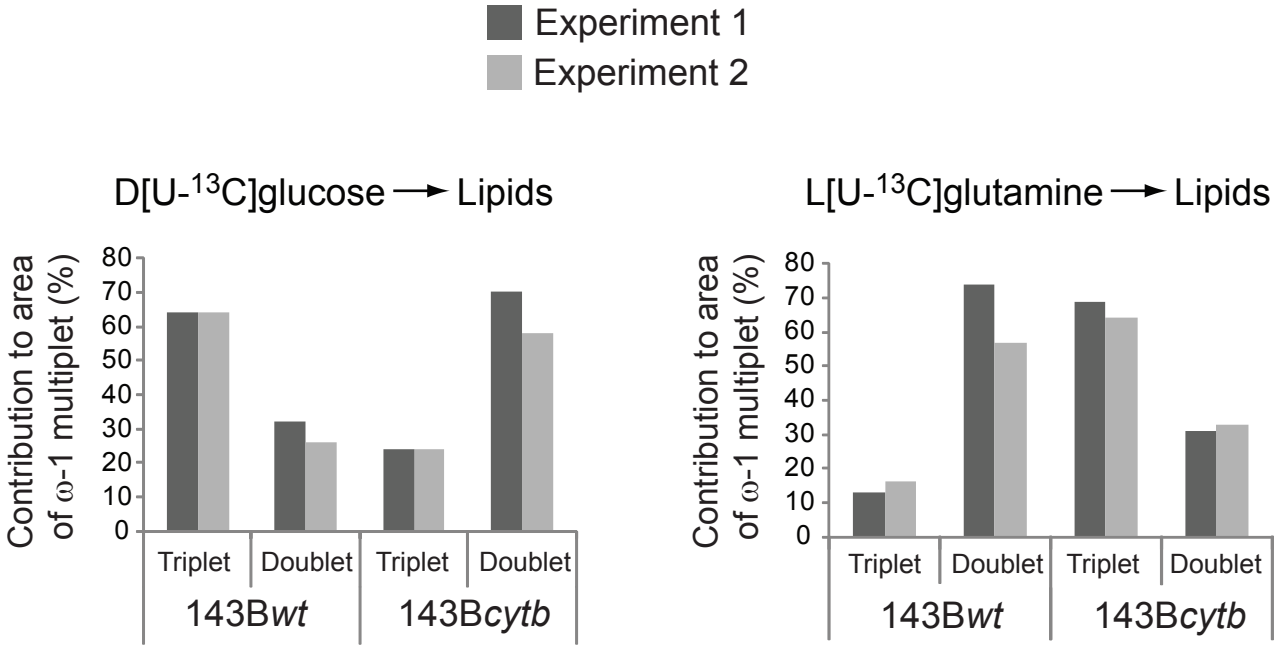

b

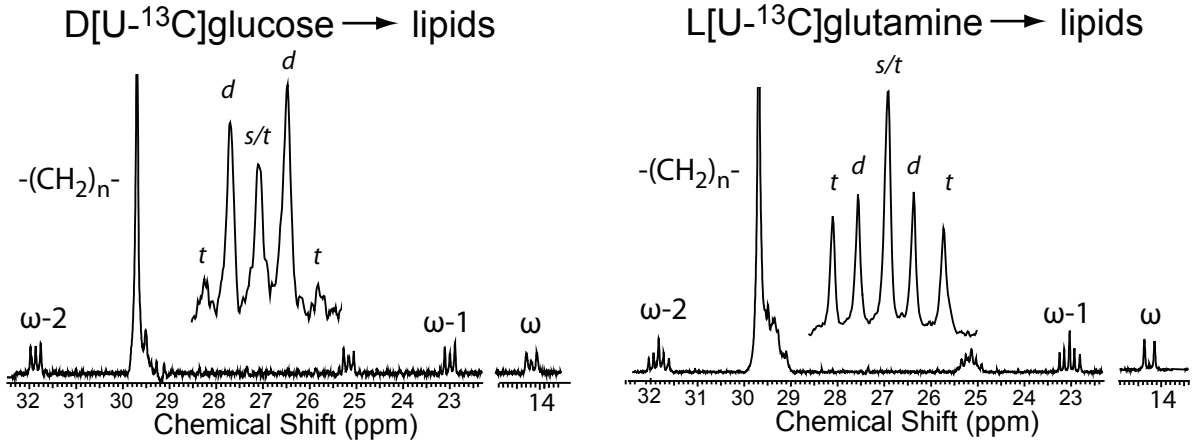

Supplementary Fig. 9

a

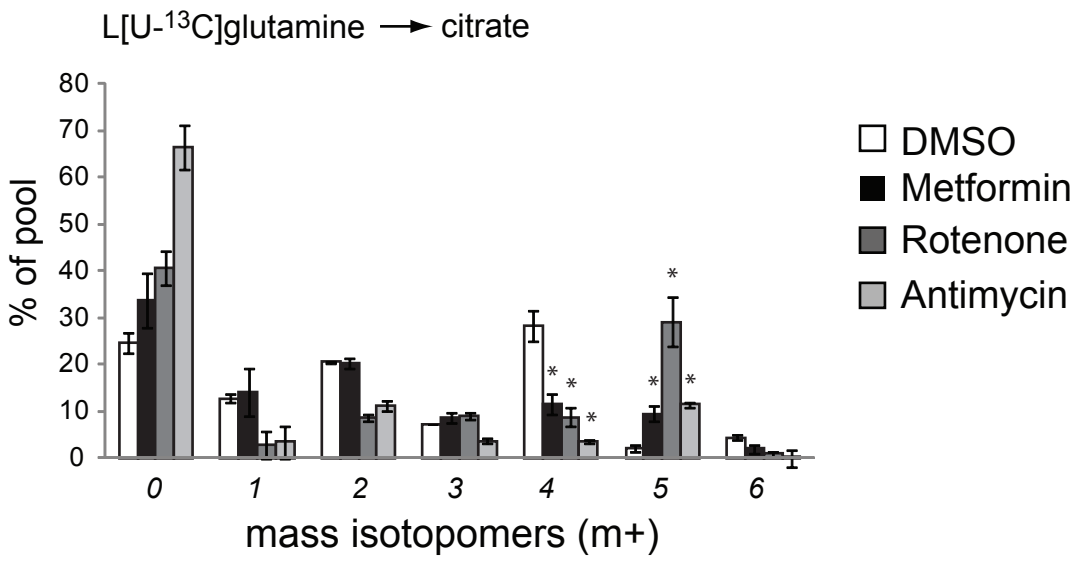

b

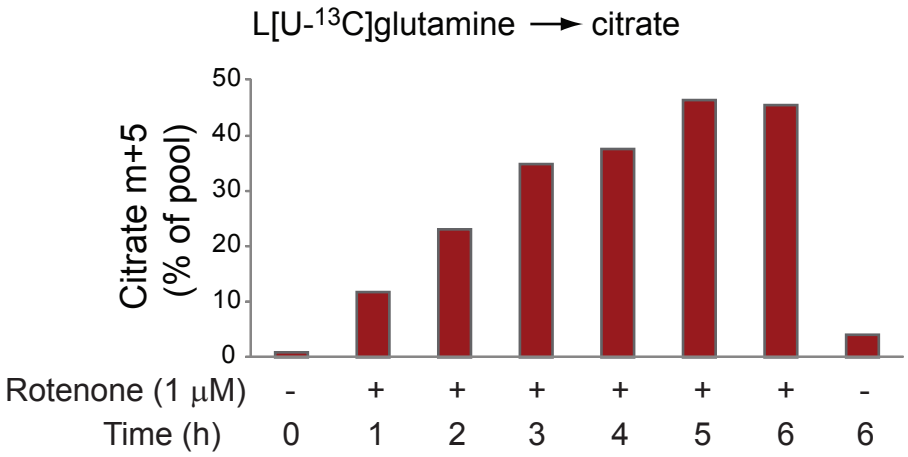

c

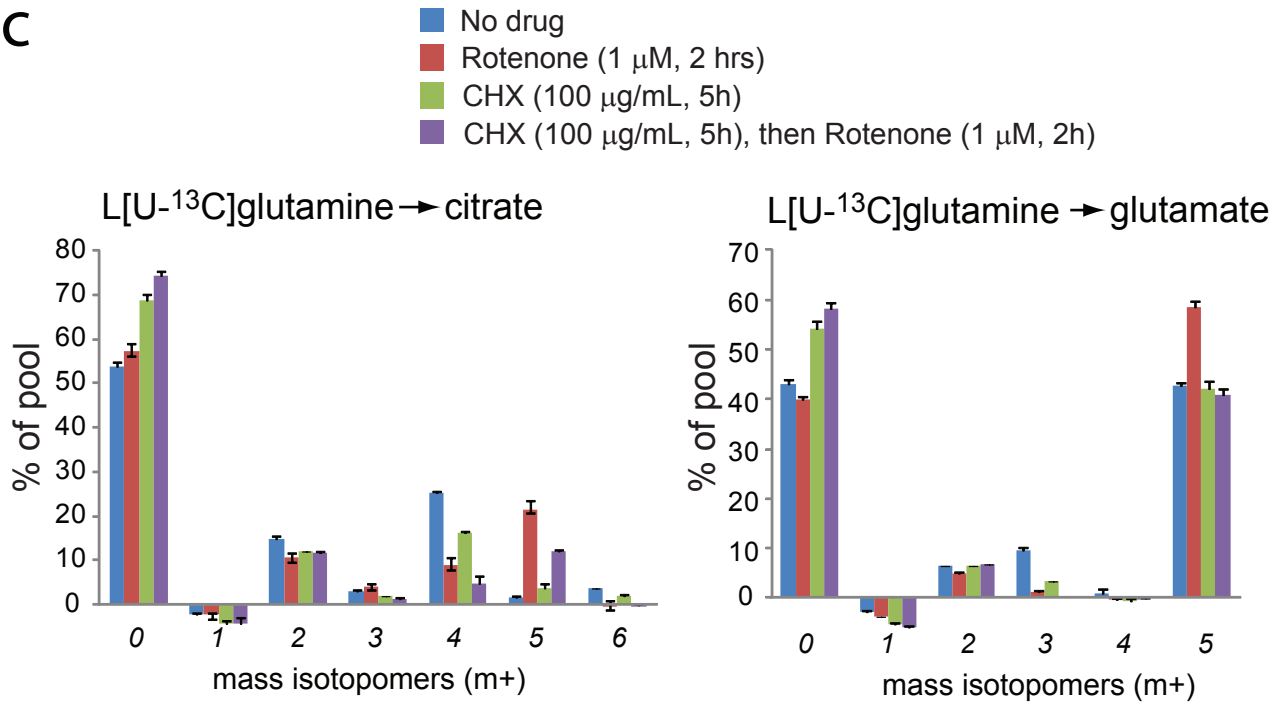

Supplementary Fig. 10